Paper pa02-063
Submitted to the 28th International Conference on High Energy Physics
ICHEP'96, Warsaw, Poland, July 1996

Leading Neutron Production in Deep Inelastic $e-p$ Scattering at HERA

H1 Collaboration

Abstract

Events with a high energy neutron emitted close to the proton beam direction have been observed in deep-inelastic $e-p$ collisions by the H1 experiment at HERA. The results are found to be in reasonable agreement with the predictions of a pion exchange model. The fraction of events with a leading neutron of energy $E_n \geq 300$ GeV is within the errors independent of Q^2 and Bjorken x in the range $2 \leq Q^2 \leq 100\,\mathrm{GeV}^2$ and $5\ 10^{-5} \leq x_{Bj} \leq 10^{-2}$. If the pion exchange model is used to correct for acceptance, $\left(7^{+7}_{-3}\right)$ % of all $e-p$ collisions and $\left(3.3^{+3.0}_{-1.0}\right)$ % of the diffractive $e-p$ collisions are determined to have a leading neutron. It is estimated that in $\left(25^{+32}_{-9}\right)$ % of the diffractive $e-p$ collisions the proton dissociates. An outlook is given onto the more detailed studies made possible by the new high resolution neutron calorimeter installed in the winter shut down of 1995/1996.

The detection of leading neutrons at HERA makes possible the study of electron scattering off the virtual meson cloud in the proton. The beam optics of HERA allow very forward scattered neutral particles within 0.8 mrad of the incident proton beam direction to be detected. The H1 collaboration has therefore installed a high resolution hadron calorimeter for 1996 data taking. During 1995, data were taken with a simple test calorimeter. Preliminary results of an analysis of these data are reported in the following. The new forward neutron calorimeter will be briefly described at the end.

The forward neutron calorimeter (FNC) is located at a distance of about 106 m from the interaction region (IR) in the HERA tunnel. The geometrical acceptance is defined by the apertures of the beam line magnets between the FNC and the IR and extends out to scattering angles θ of about 0.8 mrad over a limited region of the azimuthal angle ϕ. The overall geometrical acceptance for $\theta \leq 0.8$ mrad is estimated to $(21 \pm 5)\%$. Monte Carlo calculations [1] show that about $(30 \pm 8)\%$ of all neutrons produced by possible models of pion-exchange are within the geometrical acceptance. One also expects leading neutrons from diffractive processes in which the excited leading proton dissociates. It is estimated by Monte Carlo simulations [4] that about $(5 \pm 2)\%$ of all diffractive events with proton dissociation yield a leading neutron within acceptance of the neutron counter.

During 1995 a lead scintillator sandwich calorimeter was used. It was 1.4 m deep corresponding to $7\lambda_I$ and its transverse dimensions were 30×30 cm^2. The minimal transverse distance of a neutron impact point to an edge of the calorimeter was about 9 cm. Two scintillation counters in front of the calorimeter were used to veto charged particles. For a neutron it was demanded that neither of the two veto counters shows a signal above noise.

Fig.1 shows the energy spectrum of neutrons from deep inelastic scattering (DIS) together with the expectation from a pion exchange model obtained by Monte Carlo simulation [1]. These simulations do not include the hadronic shower in the neutron calorimeter; instead a gaussian neutron energy resolution of 20% was used. The model calculations provide a reasonable description of the data for neutron energies above 400 GeV. As incident neutrons can also cause signals in the veto counters, either by secondary particles due to interactions in the material in front of the counters, by backscattering of particles from hadronic shower in the calorimeter, or by accidental coincidences, the neutron detection probability is suppressed. It was estimated from the height of the pion exchange peak in the energy spectrum without veto requirement to be $(50 \pm 20)\%$ for neutrons of energies $E_n > 300$ GeV.

The Q^2- and x_{Bj}-dependence of the events with a detected neutron of $E_n > 300$ GeV normalised to all DIS events is shown in Fig.2. The energy threshold $E_n > 300$ GeV is applied to all neutron data shown in the following. So as not to introduce any bias, Q^2 and x_{Bj} were determined from the kinematics of the scattered positron only, requiring $E_e \geq$ 7 GeV and $Q^2 \geq 2.0$ GeV^2. Within the statistical errors the Q^2- and x_{Bj}-dependences of events with a leading neutron are similar to those of the fully inclusive DIS events. The fraction of observed leading neutron events is about 1.1%. Correcting this number for the detector acceptance assuming pion exchange and the neutron detection probability, we determine the fraction r of DIS events with a leading neutron to be $r = \left(7^{+7}_{-3}\right)\%$. This value can be compared with $r = \left(9.1^{+3.6}_{-5.7}\right)\%$ obtained by the ZEUS collaboration [5] and $r = 6.8\%$ predicted by the pion-exchange model [1].

A first look at the global characteristics of the hadronic final state are given in Fig.3, where the observed, i.e. not corrected for any detector effects, distribution of events as a function of η_{max} is given. η_{max} is the pseudo rapidity of the calorimeter cluster with an energy greater than 400 MeV closest to the proton beam direction. In Fig.3a) the distribution of the inclusive DIS events and of events with a leading neutron are given. By requiring no significant activity in the detectors adjacent to the proton remnant direction, i.e. for $\eta > 3.2$, except for the neutron calorimeter, a sample of so called "rapidity gap" events is selected, which is used in the study of diffraction in DIS [6]. The distribution of events passing these selection cuts is shown in Fig.3b). There are only 35 events with $\eta_{max} < 2$ with a leading neutron in comparison with about 10300 events with $\eta_{max} < 2$ in the full "rapidity gap" sample. Assuming for the calculation of the acceptance that these leading neutron events are due to pion exchange, we estimate a leading neutron fraction of $\left(2.3^{+1.9}_{-0.8}\right)\%$ for events of the diffractive sample with $\eta_{max} < 2.0$. Since the "rapidity gap" selection rejects with high efficiency only events with $M_Y \geq 1.6\,\mathrm{GeV}$, some of the leading neutron events in Fig.3b) are due to proton dissociation, via the excitation of the $N(1440)$ for example. The estimated pion exchange contribution is therefore more an upper limit. To estimate the relative amount of proton dissociation in diffractive scattering we use Fig.3a), thus avoiding any bias due to the "rapidity gap" selection. Assuming, as is usualy done, that the 8500 events in the interval $|\eta_{max}| < 1$ in Fig.3a) are due to diffractive scattering, which implies that the 52 leading neutron events in this interval are due to proton dissociation, we estimate, taking the corresponding acceptance and the detection probability into account, that in $\left(25^{+32}_{-9}\right)\%$ of all diffractive events the proton dissociates. The errors are dominated by the uncertainties of the neutron counter acceptances and of the detection probability.

These numbers are confirmed if one analyses the data somewhat closer following the particle exchange model depicted in Fig.4. The virtual photon interacts with a quark of the exchanged colourless particle p producing the hadronic system X. The colourless baryonic system Y, in the simplest case a proton (p = pomeron) or a neutron (p = pion) is emitted close to the proton beam direction. When both M_X and M_Y are sufficiently small, the system X and Y are forced kinematically to be separated by a rapidity gap. By measuring the mass M_X in the central detector we can, neglecting the four momentum transfer t between the incoming proton and the system Y, determine x_p and β, where $x_p \simeq x_{Bj} \cdot (Q^2 + M_X^2)/Q^2$ is the incoming proton momentum fraction carried by the exchanged particle p , and $\beta = x_{Bj}/x_p$ is the momentum fraction of the exchanged particle p carried by the interacting quark.

We restrict the further analysis to the "rapidity gap" and leading neutron samples, for which the candidate exchange particles (Regge trajectories) are the pomeron and the pion, respectively. The observed x_p-distributions are shown in Fig.5 together with the predictions of the pion-exchange model [1]. For the H1 diffractive sample usually the additional cut $x_p < 0.05$ is made. From the leading neutron events in this sample, which are also shown in Fig.5, we estimate a pion exchange fraction of $\left(3.3^{+3.0}_{-1.0}\right)\%$ for the diffractive sample $x_p < 0.05$. The system X is only for $x_p <$ 0.05 fully measured by the central detector. For larger x_p more and more particles escape detection through the beam pipe. Therefore the x_p determination via the M_X measurement, which was used for Fig.5, is inadequate for $x_p >$ 0.05 due to this loss of forward going particles.

A more direct determination of x_p would be via the leading particle energy $x_p = 1.0 - E_n/E_{beam}$. Although a neutron energy resolution of 20% is hardly adequate for such a determination, we nevertheless show in Fig.6 the x_p-distribution obtained in this way. Also shown in Fig.6 is the pion exchange model prediction. Fig.6 is of course only a simple mapping of Fig.1 with the cut $E_n > 300$ GeV corresponding to $x_p < 0.63$. The few events with $E_n > 820$ GeV resulting in negative values of x_p have been discarded.

Of central interest for this exploratory survey is of course the β-distribution, as it yields the information about the structure of the exchanged particle. Fig.7 shows the β-distributions of the data and of the pion-exchange model prediction. In Fig.7 the neutron energy has been used to determine x_p and the measured energy and scattering angle of the positron to determine x_{Bj}.

The various distributions of DIS events with a leading neutron show at least qualitatively reasonable agreement with the predictions of the pion exchange model. In this simple model [1] the pion flux of the proton and the electron-pion DIS cross section factorize. It uses the pion flux as given in [2] and the leading order pion structure functions of GRV [3]. For a more detailed comparison between data and theoretical predictions and for a deeper study in general [7] one would like to have β-distributions in bins of x_p and t. This clearly needs a calorimeter with a good energy and angular resolution. We expect the new neutron calorimeter installed during the last winter shut down replacing the test calorimeter of 1995, to fulfil these requirements.

The design of the new FNC is based on a compensating lead/scintillating fibre calorimeter built originally by the LAA project at CERN and subsequently used by the WA89 collaboration (see [9],[10], and references therein). The calorimeter consists of 75 hexagonal towers of a height of about 7.5 cm and a depth of 2 m. In front of the calorimeter two planes of hodoscope tiles with the same granularity as the calorimeter are mounted.

Fig.8 shows a front view of the detector. The hexagonal tower structure of the device is visible. The hatched circle in the upper part indicates the position of the HERA proton beam pipe. The other hatched area corresponds to the impact region of neutrons from deep inelastic e-p scattering. The lateral dimensions of the calorimeter as well as the depth of $9.5\lambda_I$ ensures a containment for hadronic showers of more than 95 % even for the highest energies. At the end of last year the device was tested in a 15 GeV/c pion test beam at CERN. The results suggest that, without further corrections, the resolution can be described by $\sigma_E/E = (64.2/\sqrt{(E[GeV])} + 2.5)\%$ where the constant term has been taken from the LAA results. One of the main advantages of the high granularity of the device is the possibility to reconstruct the neutron impact point with high accuracy. The measured resolution is in good agreement with previous measurements from the LAA collaboration and can be parametrised by $\sigma_y[mm] = 33.3/\sqrt{(E[GeV])} + 2.4$ where the constant term has again been taken from the previous LAA measurements. To maintain these resolutions in a hostile environment like the HERA tunnel is an experimentally challenging task.

Acknowledgements

We are grateful to the HERA machine group whose outstanding efforts have made and continue to make this experiment possible. We thank the engineers and technicians for their work in constructing and now maintaining the H1 detector, our funding agencies for financial support, the DESY technical staff for continual assistance, and the DESY directorate for the hospitality which they extend to the non–DESY members of the collaboration.

References

[1] The pion-exchange version of the "Rap-Gap" Monte Carlo generator was used; H. Jung, Comp. Phys. Comm. 86 (1995), and to be published. It uses the pion flux of the proton given in [2] and the leading order pion structure functions of GRV [3].

[2] W. Koepf,L.L. Frankfurt and M. Strikman, Phys. Rev. 53 (1996) 2586

[3] M. Glück,E. Reya and A. Vogt,Z. Phys. C 53 (1992) 651

[4] B. List, Diplomarbeit TU-Berlin, H1-Note H1-10/93-319 unpublished

[5] ZEUS-Collaboration, M. Derrick et al., DESY 96-063, March 1996

[6] H1-Collaboration, T. Ahmed et al., Phys. Lett. B 348 (1995) 681

[7] B. Kopeliovich, B. Povh and I. Potashnikova, DESY 96-011, January 1996

[8] T. Nunnemann, Diplomarbeit, Univ. Heidelberg, 1996, unpublished

[9] M. Livan, V. Vercesi, R. Wigmans, "Scintillating Fiber Calorimetry", CERN Yellow Report 95-05, CERN 1995, and ref. therein

[10] C. Scheel, PhD Thesis, University of Amsterdam, 1994, unpublished

Figure 7: The β distributions deduced from the observed values of x_{Bj} and E_n (full circles) together with the pion-exchange model pridiction (histogram). The normalization is to the number of events.

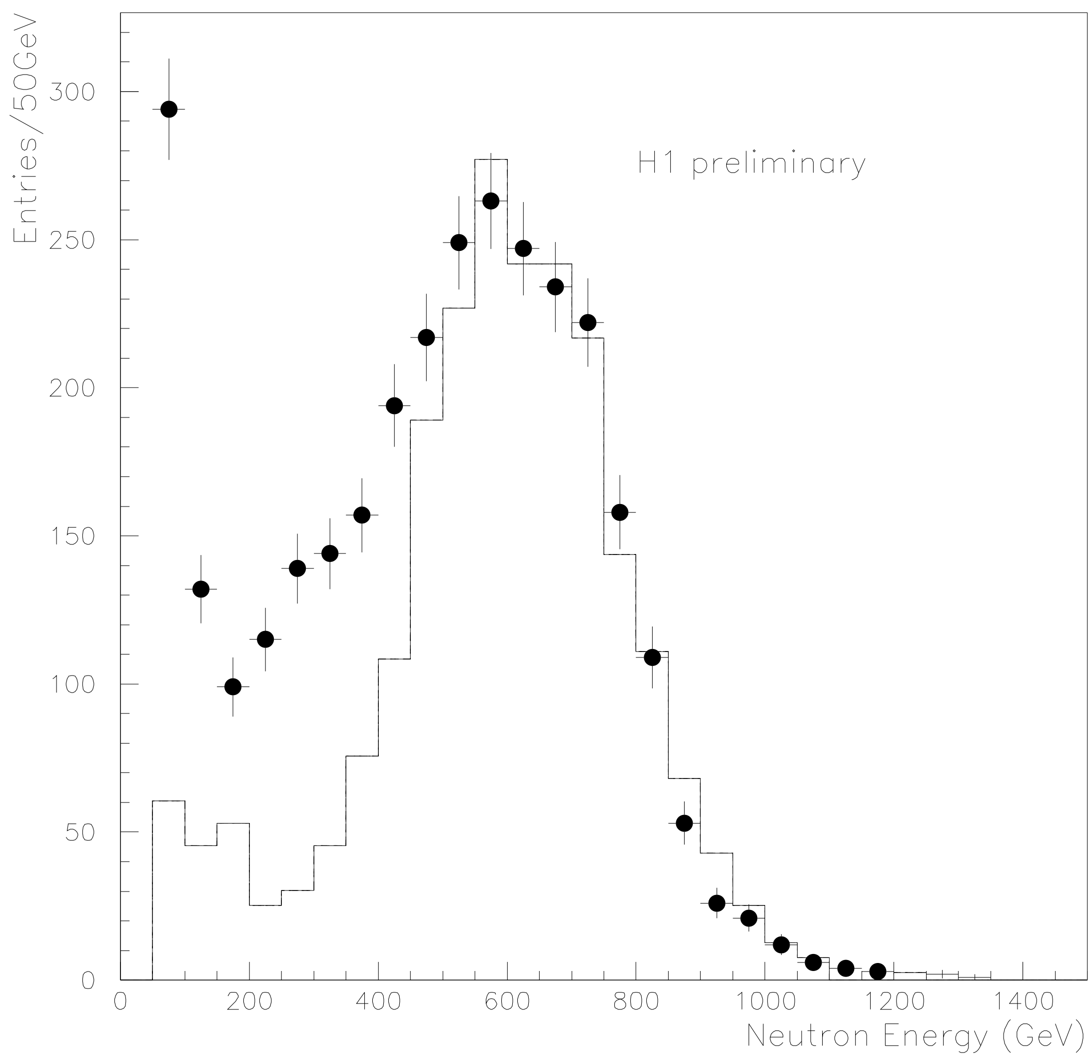

Figure 1: The observed neutron energy distribution. The histogram results from a Monte Carlo simulation based on a pion exchange model using a gaussian neutron energy resolution of 20%. The normalization is to the peak height.

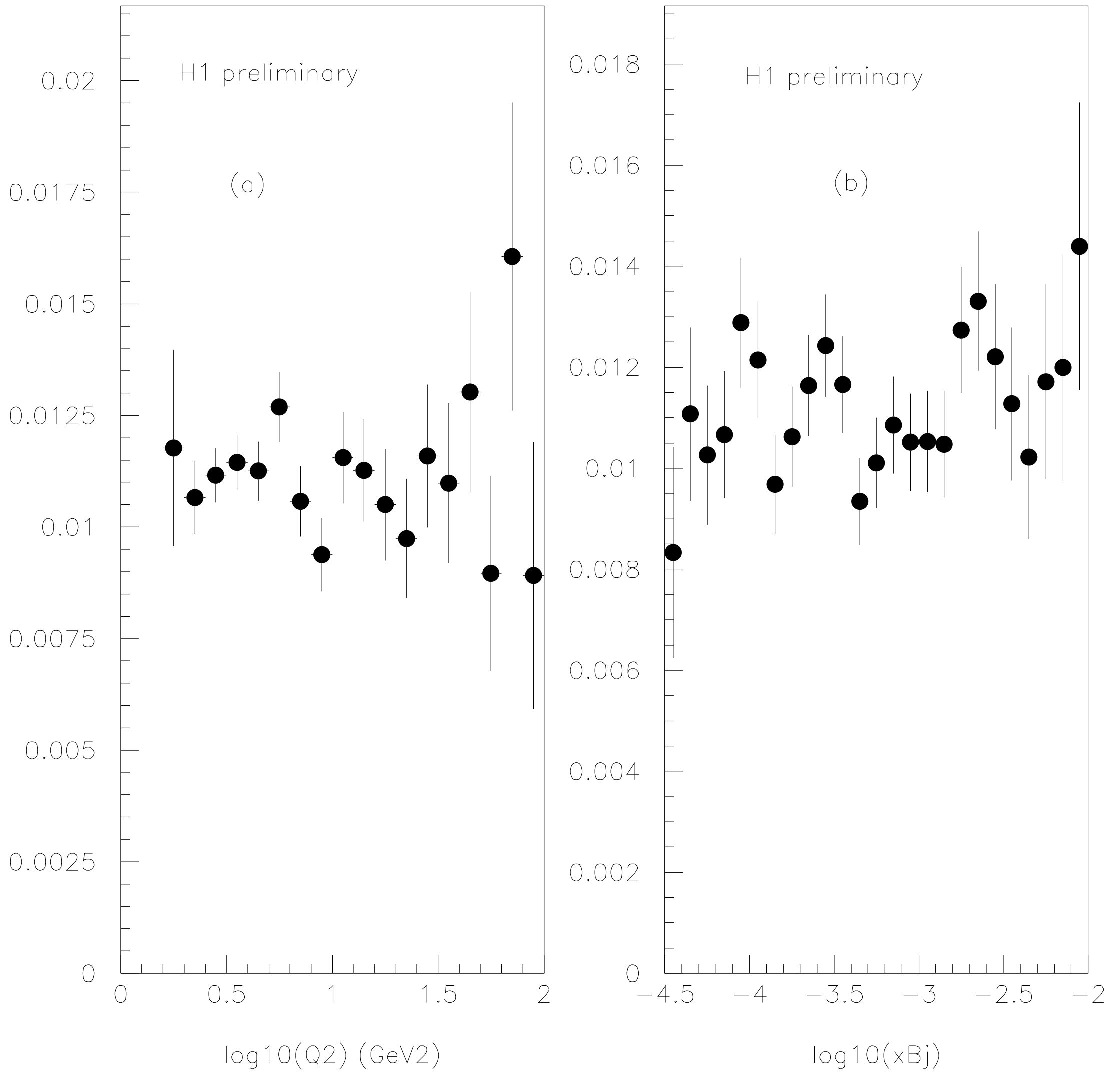

Figure 2: The observed ratio of leading neutron events to all DIS events as a function of (a) Q^2 and (b) x_{Bj}.

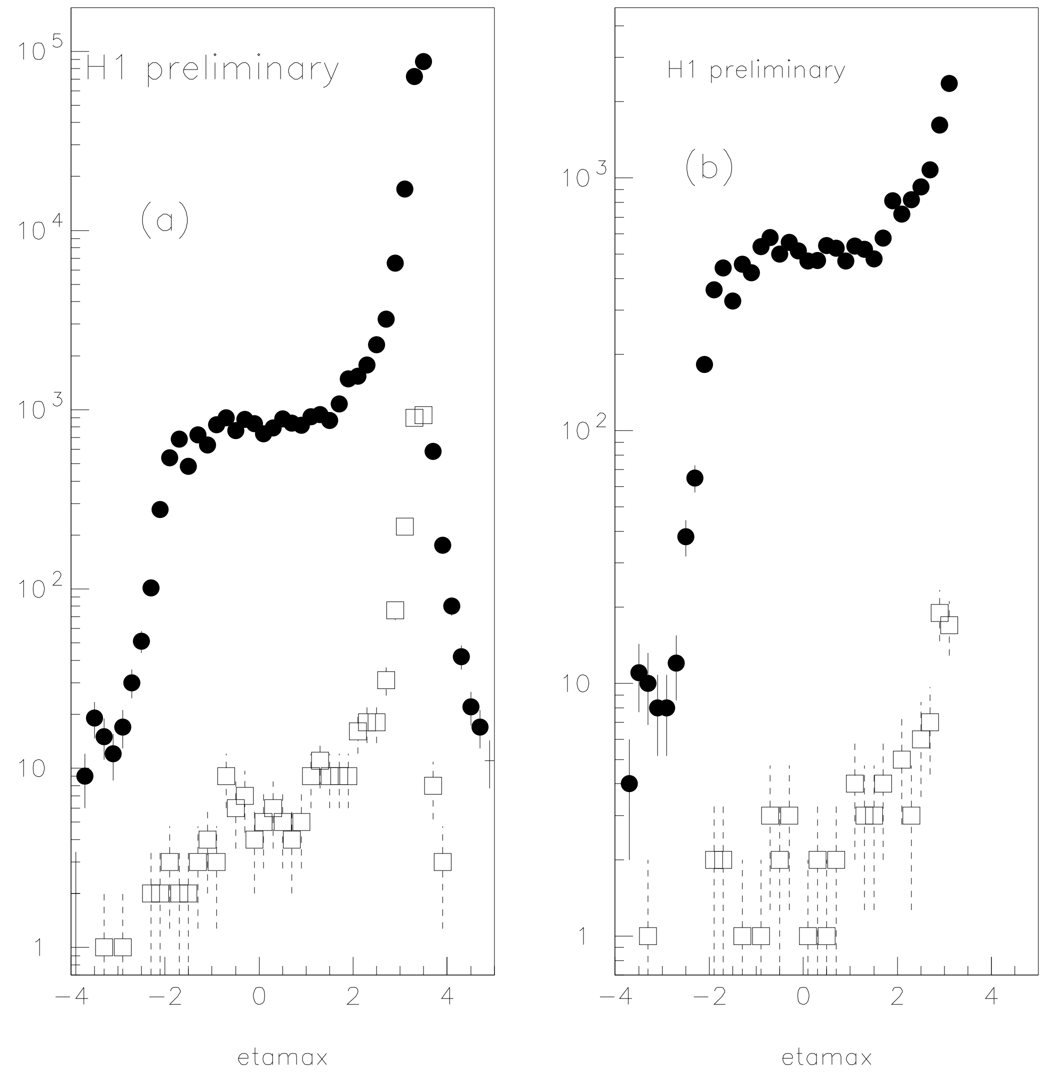

Figure 3: The observed η_{max}-distributions. In (a) for all DIS events (full circles) and leading neutron event (open sqares). In (b) only those events are shown which pass the diffraction selection cuts, the so called “rapidity gap”- sample.

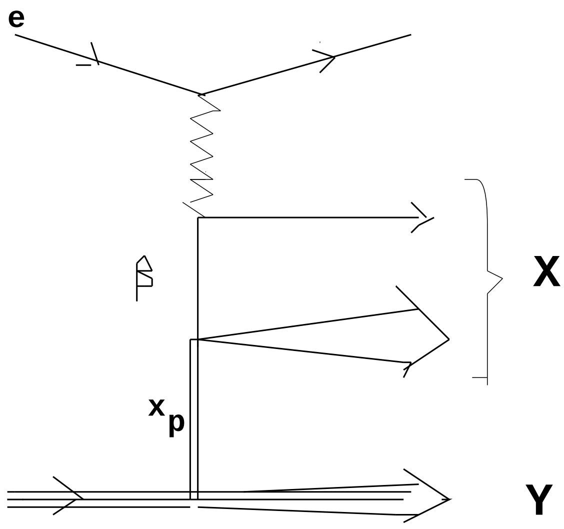

Figure 4: The particle exchange diagram. x_p is the proton momentum fraction carried by the exchanged particle p, and β is the momentum fraction of the particle p carried by the interacting quark.

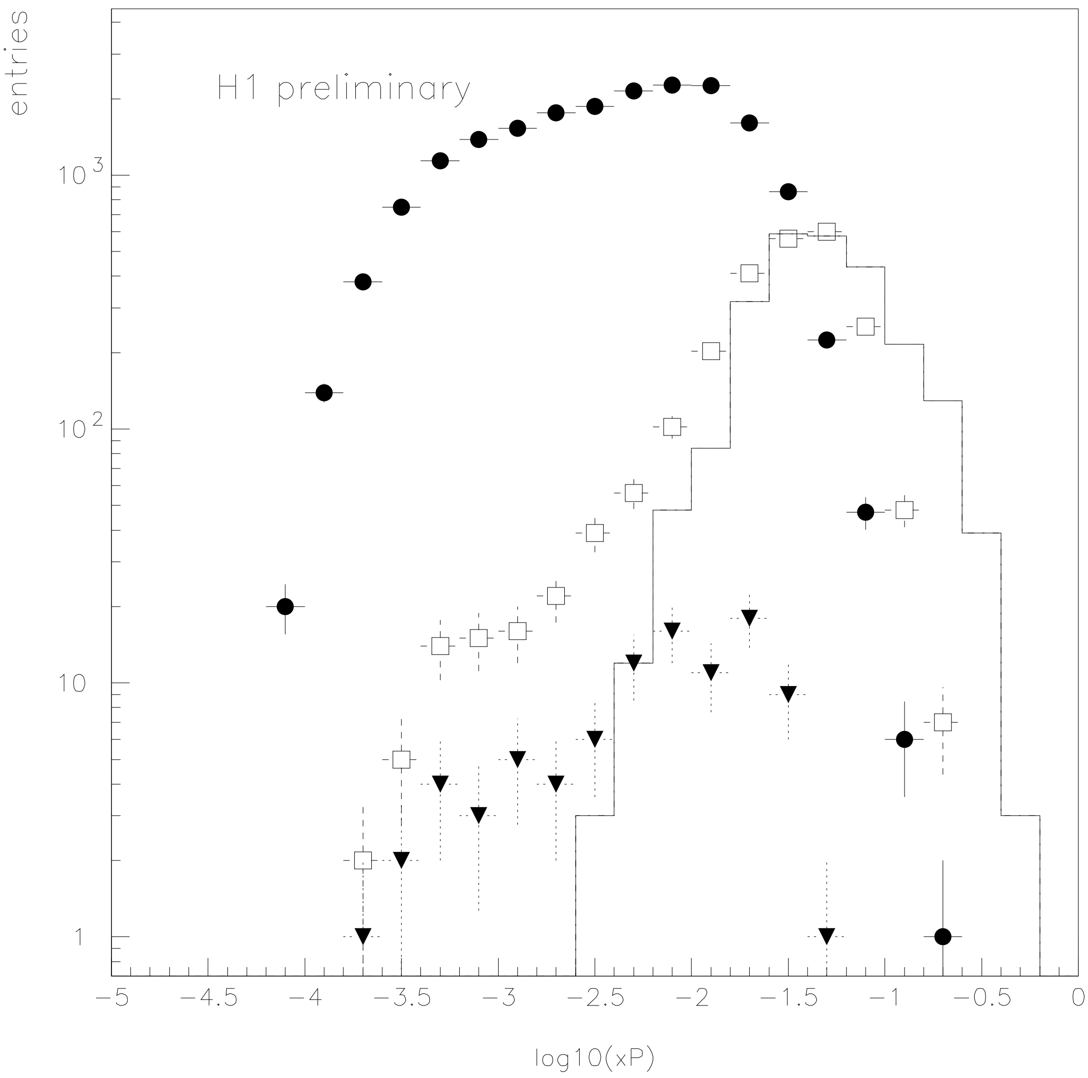

Figure 5: The x_p distributions of the "rapidity gap" sample (full circles) and the leading neutron events (open sqares) deduced from the observed values of x_{Bj}, Q^2, and M_X. The leading neutron events of the diffractive sample are shown as full triangles. The pion-exchange model results are shown as a histogram normalized to the peak height of the leading neutron events.

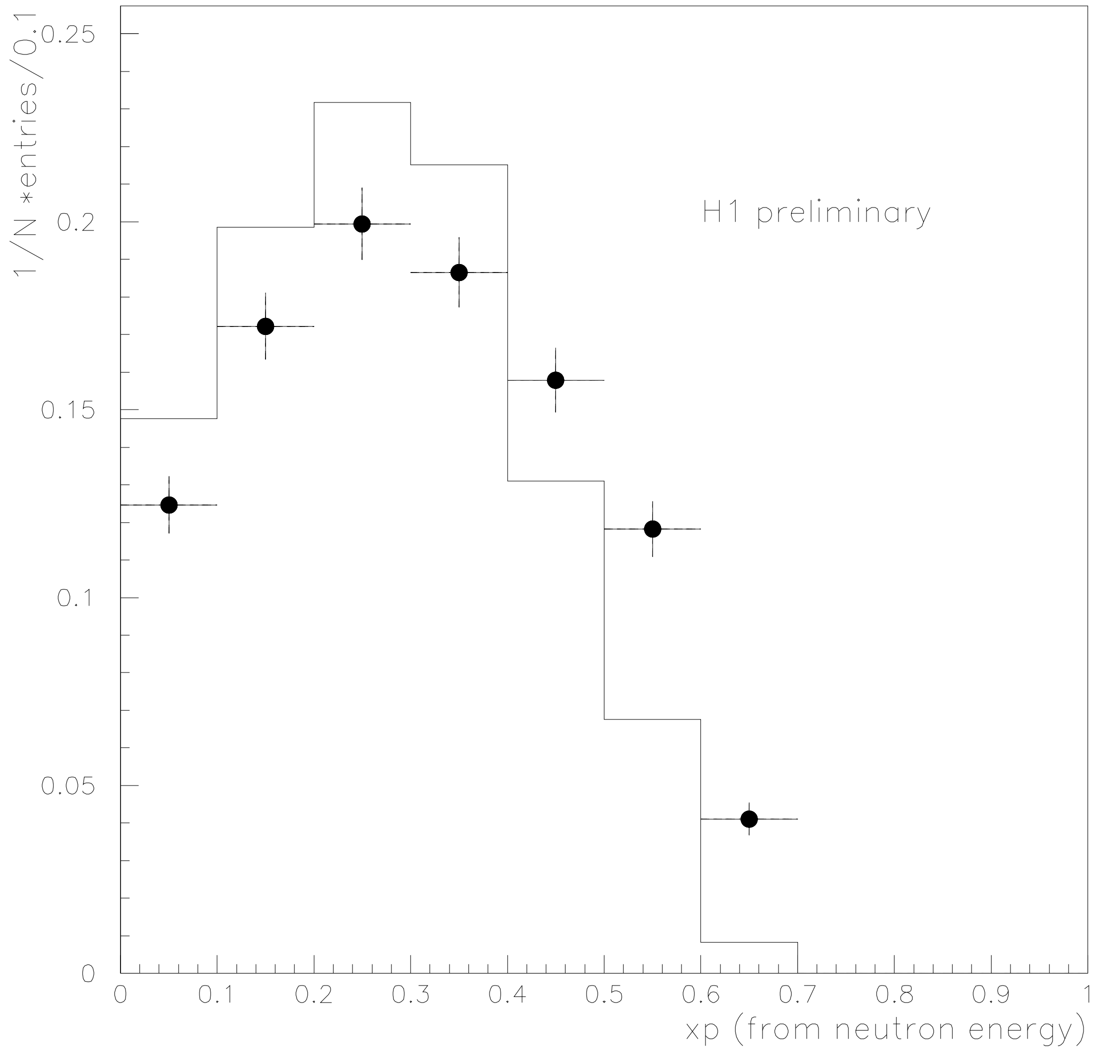

Figure 6: The x_p distributions deduced from the measured neutron energy (full circles) together with the pion-exchange model prediction (histogram). The normalization is to the number of events.

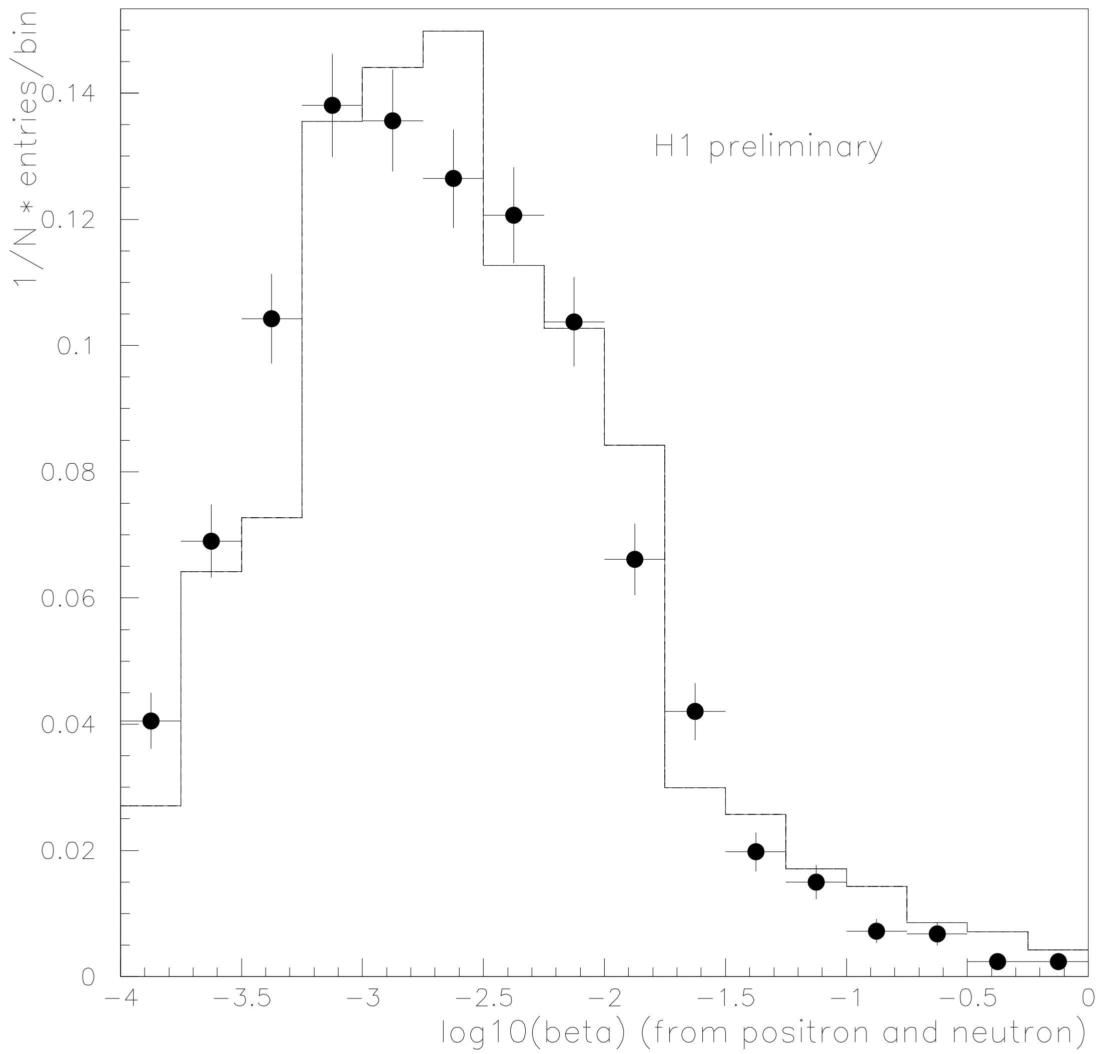

is to the number of events.

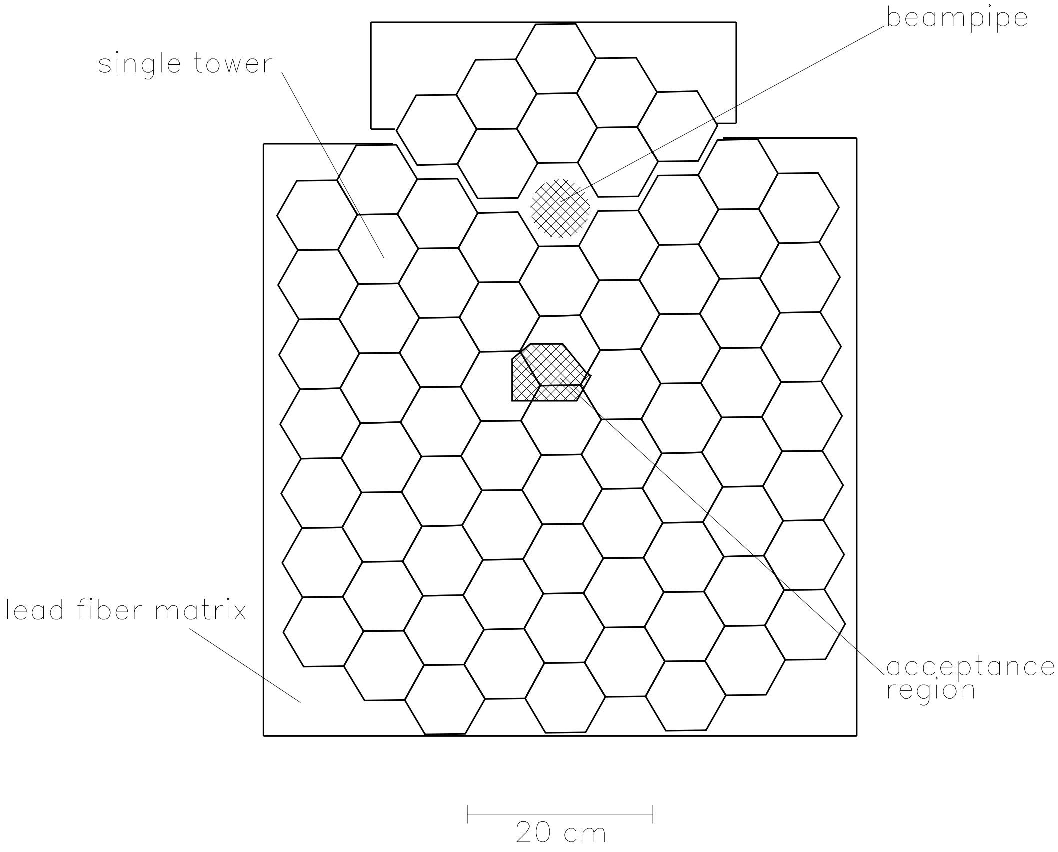

Figure 8: Front view of the new FNC. The beam pipe and the neutron acceptance region are indicated as hatched areas.